JOURNAL

OF THE AMERICAN CHEMICAL SOCIETY

© Copyright 1985 by the American Chemical Society

VOLUME 107, NUMBER 8 APRIL 17, 1985

Studies on the Photochemistry of Chromium Hexacarbonyl in the Gas Phase: Primary and Secondary Processes

T. Rick Fletcher and Robert N. Rosenfeld*

Contribution from the Department of Chemistry, University of California, Davis, Davis, California 95616. *Received August 30, 1984*

Abstract: The photochemistry of $Cr(CO)_6$, induced by pulsed laser excitation at 249 nm, has been studied with time resolved infrared laser absorption spectroscopy. This method allows us to determine the temporal evolution of the reactant and all major product species. We find that photoactivated $Cr(CO)_6$ decays to yield $Cr(CO)_5$ and CO. The CO product is translationally as well as ro-vibrationally excited. The $Cr(CO)_5$ product is formed with sufficient internal energy to undergo rapid dissociation, yielding $Cr(CO)_4$ and CO. Both decarbonylation reactions occur within 10^{-7} s of the photoactivation laser pulse. $Cr(CO)_4$ reacts with $Cr(CO)_6$ at a rate of 1.8 ($\pm$0.3) $\times$ 10^7 $torr^{-1}$ s^{-1}, yielding $Cr_2(CO)_{10}$. This binuclear complex has a lifetime of at least 10^{-3} s under our experimental conditions. $Cr(CO)_4$ reacts with CO to form $Cr(CO)_5$ at a rate of 1.4 ($\pm$0.2) $\times$ 10^6 $torr^{-1}$ s^{-1}. $Cr(CO)_5$ reacts with CO to form $Cr(CO)_6$ at a rate of 1.2 ($\pm$0.2) $\times$ 10^6 $torr^{-1}$ s^{-1}.

The photochemistry of transition-metal carbonyls and the structure and reactivity of the coordinatively unsaturated fragments derived from these species have been the focus of many recent investigations.[1-5] This interest is due in large part to the central role which metal carbonyls appear to play in the photocatalysis of reactions such as olefin isomerization, oligomerization, and hydrogenation. Elucidation of the relevant catalytic mechanisms requires, however, a more complete data base on the photophysics and photochemistry of metal carbonyls and the kinetics, both unimolecular and bimolecular, of the reactions of their dissociation products. We have begun to obtain such data for the molecule chromium hexacarbonyl, $Cr(CO)_6$, using time-resolved spectroscopic techniques. Preliminary results[6] previously reported have been re-investigated and extended. An essentially complete mechanistic picture emerges which will be detailed in this paper.

Previous work on the photochemistry of metal carbonyls and the structure and reactivity of unsaturated metal centers can be broadly categorized as "chemical" or "physical". Examples of the former include studies of substituent effects on photosubstitution yields and rates,[7b] attempts to stabilize reactive intermediates using bulky substituents,[7] and the chemical trapping of reactive intermediates[4] as diagnostic tools. Such studies have made a substantial contribution to the development of mechanistic models in metal carbonyl photochemistry; however, data from more direct, "physical" probes are clearly required if these models are to be refined. Thus, various spectroscopic methods have recently been employed in characterizing the elementary dissociative steps in metal carbonyl photochemistry and the structure of the coordinatively unsaturated reactive intermediates thus formed. Turner and co-workers[8] have made important contributions in this regard, using cryogenic matrix isolation methods to obtain electronic and vibrational spectroscopic data on various species, $M(CO)_n$ (M = Fe, Cr, Ni, etc.). Matrix methods are not, however, well-suited for studying the kinetics of bimolecular reactions. Various flash photolytic methods have been used to characterize the spectra and lifetimes of reactive intermediates formed by the photodissociation of metal carbonyls.[3,9,10] Especially noteworthy are the picosecond absorption studies of the solution phase photofragmentation of $Cr(CO)_6$ by Peters, Vaida, and co-workers,[11] and the infrared absorption studies of $Fe(CO)_5$ photodissociation products in the gas phase by Weitz and co-workers.[12] A large body of evidence

(1) (a) Geoffroy, G. L.; Wrighton, M. S. "Organometallic Photochemistry"; Academic Press: New York, 1979. (b) Wrighton, M. S. *Chem. Rev.* **1974**, *74*, 401.

(2) (a) Whetten, R. L.; Fu, Ke-Jian; Grant, E. R. *J. Chem. Phys.* **1982**, *77*, 3769. (b) Whetten, R. L.; Fu, Ke-Jian; Grant, E. R. *J. Am. Chem. Soc.* **1982**, *104*, 4270.

(3) Hermann, H.; Grevels, F.; Henne, A.; Schaffner, K. *J. Phys. Chem.* **1982**, *86*, 5151.

(4) (a) Yardley, J. T.; Gitlin, B.; Nathanson, G.; Rosan, A. M. *J. Chem. Phys.* **1981**, *74*, 361. (b) Nathanson, G.; Gitlin, B.; Rosan, A. M.; Yardley, J. T. *J. Chem. Phys.* **1981**, *74*, 370. (c) Tumas, W.; Gitlin, B.; Rosan, A. M.; Yardley, J. T. *J. Am. Chem. Soc.* **1982**, *104*, 55.

(5) (a) Turner, J. J.; Burdett, J. K.; Perutz, R. N.; Poliakoff, M. *Pure Appl. Chem.* **1977**, *49*, 271. (b) Burdett, J. K.; Turner, J. J. "Cryogenic Chemistry"; Ozin, G. A., Ed.; Wiley: New York, 1976.

(6) Fletcher, T. R.; Rosenfeld, R. N. *J. Am. Chem. Soc.* **1983**, *105*, 6358.

(7) (a) Bradley, D. C. *Adv. Chem. Ser.* **1976**, *150*, 266. (b) Lappert, M. F. *Adv. Chem. Ser.* **1976**, *150*, 256. (c) Bradley, D. C. *Chem. Br.* **1975**, *11*, 393.

(8) (a) Perutz, R. N.; Turner, J. J. *J. Am. Chem. Soc.* **1975**, *97*, 4800. (b) Burdett, J. K.; Graham, M. A.; Perutz, R. N.; Poliakoff, M.; Rest, A. J.; Turner, J. J.; Turner, R. F. *J. Am. Chem. Soc.* **1975**, *97*, 4805. (c) Perutz, R. N.; Turner, J. J. *J. Am. Chem. Soc.* **1975**, *97*, 4791. (d) Perutz, R. N.; Turner, J. J. *Inorg. Chem.* **1975**, *14*, 262.

(9) Breckenridge, W. H.; Sinai, N. *J. Phys. Chem.* **1981**, *85*, 3557.

(10) Wegmen, R. W.; Olsen, R. J.; Gard, L. R.; Faulkner, L. R.; Brown, T. L. *J. Am. Chem. Soc.* **1981**, *103*, 6089.

(11) (a) Welch, J. A.; Peters, K. S.; Vaida, V. *J. Am. Chem. Soc.* **1982**, *86*, 1941. (b) Simon, J. D.; Peters, K. S. *Chem. Phys. Lett.* **1983**, *98*, 53.

0002-7863/85/1507-2203$01.50/0 © 1985 American Chemical Society

indicates that qualitatively different products are formed following the photolysis of metal carbonyls in solution than in the gas phase. Fragments formed by the cleavage of a *single* metal–CO bond are characteristically produced upon solution phase photolysis[1] while in the gas phase more extensive fragmentation, yielding di-, tri-, and tetra-unsaturated metal carbonyls, is typically observed.[4,12,13] Thus, gas-phase studies permit data to be obtained on the structure and reactivity of reactive intermediates which are inaccessible in solution. Additionally, mono-unsaturated metal carbonyls are highly reactive species which rapidly bind even "inert" solvents, e.g., cycloalkanes.[14] This complexation can strongly perturb the structure and kinetics of the nominally unsaturated metal carbonyl. Thus, earlier nanosecond and microsecond flash photolysis studies of metal carbonyls in solution must be interpreted with caution. Finally, another reason for considering the gas-phase photochemistry of metal carbonyls has been suggested by the studies of Grant and co-workers,[2] who report that metal carbonyls with two or more vacant coordination sites are more effective than simple mono-unsaturated species in catalyzing olefin isomerization and hydrogenation.

We describe here the results of a series of flash photolysis experiments on $Cr(CO)_6$ in the gas phase. Time resolved infrared absorption spectroscopy is used to directly measure the rates of formation and decay of the products and reactant. The data obtained demonstrate that, in the absence of collisions, $Cr(CO)_4$ is the principal polyatomic product and is formed by two sequential decarbonylation steps. Marked differences are observed in the dissociation dynamics for the two decarbonylation reactions. $Cr(CO)_4$ is found to undergo rapid association reactions with CO and $Cr(CO_6)$, and rate constants for these processes have been determined. In particular, clustering to yield bimetallic species is observed to be a significant reaction under some conditions. Our results are discussed in light of other studies on transition-metal carbonyls, below.

Experimental Section

The instrumentation employed in our experiments has been previously described in detail.[15,16] Briefly, $Cr(CO)_6$, either neat or mixed with an added gas, is contained in a Pyrex absorption cell of path length 12–100 cm, equipped with two CaF_2 windows. Static or slowly flowing samples are employed and control experiments indicate no interference from the build up of photolysis products under our experiental conditions. The sample is photoactivated with a rare gas–halide excimer laser (Lambda Physik EMG 101) operating at ca. 2 Hz on the KrF* transition at 249 nm. The laser pulse width is nominally 20 ns, and fluences of 0.5–1.5 mJ/cm^2 are typically employed. The output of a continuous wave carbon monoxide laser is directed through the absorption cell coaxially with respect to the KrF* laser beam and then onto an infrared detector. The CO and KrF* laser beams are combined prior to entering the absorption cell and separated after exiting the cell with dichroic mirrors. Great care is taken to ensure that the two laser beams are rigorously coaxial over the entire length of the absorption cell. This is accomplished by using variable iris diaphragms in conjunction with a HeNe alignment laser. Subsquently, the relative alignment of the CO and KrF* laser beams is "tweaked" up so as to simultaneously minimize the rise time for the transient absorption signal due to the CO photoproduct and maximize its amplitude (vide infra). It was found to be crucial that the two laser beams be aligned as described in order to obtain meaningful, reproducible results. If this procedure is not carefully followed, the apparent rise times and amplitudes of transient absorption signals may deviate qualitatively from their actual values. Previously reported[6] differences in results from those described here are due to laser alignment problems.

The CO laser used in the present experiments is grating tuneable and actively stabilized. Laser line wavelengths are determined with a 0.6-m monochromator. The laser tube, which is cooled to 77 K along the entire active length, was built and operated as described by Djeu[17] to optimize performance on the (1,0) vibrational transition of CO where ca. 10 mW of output (TEM_{00}) could be routinely obtained. Without changing laser optics, output on any of several P-branch lines in the vibrational bands (1,0) to (12,11), corresponding to approximately 2100–1830 cm^{-1}, could be selected. Irradiation of a sample containing $Cr(CO)_6$ at 249 nm results in a transient change in the CO laser intensity reaching an infrared detector. Depending on the CO laser wavelength, either attenuation (absorption) or enhanced transmission could be observed. Control experiments demonstrate that none of the transients reported here are due to thermal lensing.[18] The infrared detector used in this work is a 2 mm diameter InSb element operated at 77 K. A custom designed preamplifier is employed to give an overall detector system rise time of $\lesssim$100 ns. The amplified detector signal is digitized with a 100-MHz transient recorder (Biomation 8100), and the digitized signal is stored in a microcomputer for signal averaging and subsequent plotting. In most cases, data are obtained by averaging 50–100 transients. The $Cr(CO)_6$ was obtained from Strem Chemical Co. It was normally sublimed and stored under vacuum prior to use although identical results were obtained with samples which had not been sublimed. All gases used were obtained from Matheson and were determined to be at least 99.5% pure by gas chromatography and infrared spectroscopy. Partial pressures of reagents in the absorption cell were measured with a capacitance manometer (p = 0.001–10 torr) or an oil manometer (p > 10 torr).

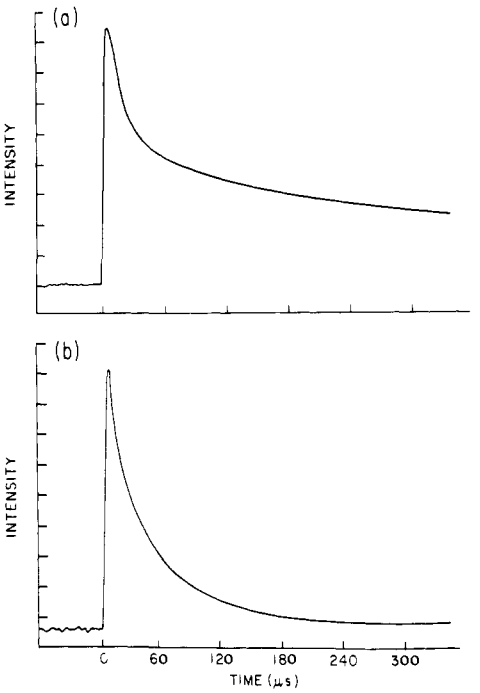

Figure 1. Time-resolved CO absorption observed following the 249-nm photolysis of $Cr(CO)_6$: (a) absorption by CO in v = 0, detected by using the $P_{1,0}(10)$ CO laser line; (b) absorption by CO in v = 1, detected by using the $P_{2,1}(10)$ CO laser line.

Results

The irradiation of metal carbonyls with high-power ultraviolet (UV) lasers has previously been observed to yield electronically excited species, e.g., metal atoms, which emit in the visible.[19,20] In fact, during the course of the present work, we have observed Cr atom emission following the excitation of $Cr(CO)_6$ at 193 or 308 nm (using fluences of ca. 1–5 mJ/cm^2). Energetic considerations indicate that such emission must be the result of multiphoton absorption. No visible emission is observed, however, upon the 249-nm excitation of $Cr(CO)_6$ at fluences $\lesssim$5 mJ/cm^2. The electronic transition excited at this wavelength is predominantly $^1A_{1g} \rightarrow d^1T_{1u}$, which is metal-to-ligand ($M \rightarrow \pi^*CO$) charge transfer in character. The 249-nm photons have an energy of ca. 115 kcal/mol while the $(CO)_5Cr–CO$ bond dissociation

(12) Ouderkirk, A.; Wermer, P.; Schultz, N. L.; Weitz, E. *J. Am. Chem. Soc.* **1983**, *105*, 3354. Ouderkirk, A. J.; Weitz, E. *J. Chem. Phys.* **1983**, *79*, 1089.
(13) Leopold, D. G.; Vaida, V. *J. Am. Chem. Soc.* **1984**, *106*, 3720.
(14) Kelly, J. M.; Long, C.; Bonneau, R. *J. Phys. Chem.* **1983**, *87*, 3344.
(15) Sonobe, B. I.; Fletcher, T. R.; Rosenfeld, R. N. *Chem. Phys. Lett.* **1984**, *105*, 322.
(16) Sonobe, B. I.; Fletcher, T. R.; Rosenfeld, R. N. *J. Am. Chem. Soc.* **1984**, *106*, 4352.
(17) Djeu, N. *Appl. Phys.* **1973**, *23*, 309.
(18) Siebert, D. R.; Grabiner, F. R.; Flynn, G. W. *J. Chem. Phys.* **1974**, *60*, 1564.
(19) Karny, Z.; Naaman, R.; Zare, R. N. *Chem. Phys. Lett.* **1978**, *59*, 33.
(20) Gerrity, D. P.; Rothberg, L. J.; Vaida, V. *J. Phys. Chem.* **1983**, *87*, 2222.

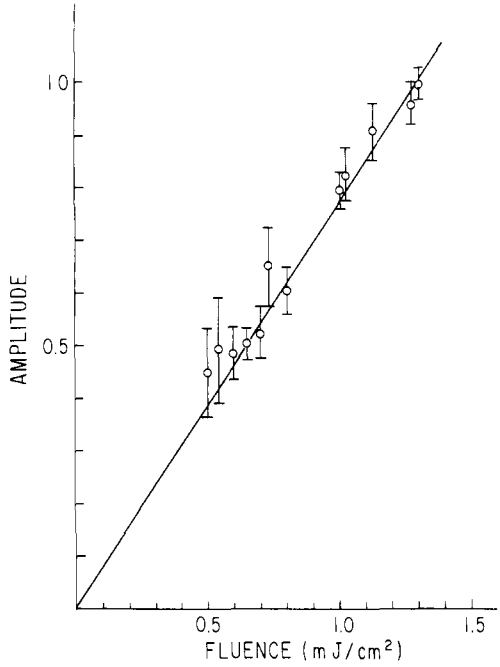

Figure 2. Dependence of CO laser absorption amplitude on KrF* laser intensity. The data were obtained by using the $P_{1,0}(10)$ CO laser line at 3.0 μs following the KrF* laser pulse. The solid line is a weighted least-squares fit to the data. A linear intensity dependence is also observed when data are taken 0.8 μs following the KrF* laser pulse.

energy is ca. 37 kcal/mol.[21] Thus, CO is produced by the photodissociation of $Cr(CO)_6$, and the yield of CO at any given time following the UV laser pulse should vary linearly with UV laser intensity, assuming CO production is the result of a single photon absorption event. Typical CO laser absorption signals due to the CO photoproduct are shown in Figure 1. Signal amplitudes at several selected times following the UV laser pulse were found to vary linearly with UV laser intensity. See Figure 2. This observation, especially in light of the relatively low UV laser fluences employed here, suggests that the chemistry which occurs is the result of a single photon absorption process. In addition, the observed extent of fragmentation [i.e., $Cr(CO)_4$, but no $Cr(CO)_3$, is formed] is also consistent with this hypothesis. Although the occurrence of multiphoton processes cannot rigorously be ruled out, such phenomena are not required to explain our results.

Transient infrared absorption following the 249-nm photoactivation of $Cr(CO)_6$ can be observed by using virtually any CO laser line over the range 2100–1900 cm^{-1}. Time-resolved absorption curves obtained by using various CO laser lines are characterized by different temporal and pressure dependences. Such observations, together with reported data[8] on the infrared absorption spectra of matrix-isolated species, $Cr(CO)_n$ (n = 3–6), provide sufficient information for the assignment of these transient absorptions.

Discussion

Following the 249-nm photolysis of $Cr(CO)_6$ in the gas phase, transient infrared absorption can be observed in five distinct spectral ranges, designated I–V in Figure 3. We have assigned absorptions in these regions to CO, $Cr(CO)_n$ (n = 4–6), and to bimetallic clusters, $Cr_2(CO)_{10}$. In general, assignments are made on the basis of reported matrix-isolated spectra,[5,8] the observed temporal dependence of a transient, and the [$Cr(CO)_6$, CO, etc.] pressure dependence of a transient. *All* of the transients observed here can be assigned in this way. Actual spectra (absorption intensity vs. CO laser frequency) can be obtained from our data but are not reported. Vibrational band contours for polyatomics in the gas phase are typically 10–20 cm^{-1} wide. Bandwidths and peak positions depend on the extent of rovibrational excitation of the species being observed. CO laser line widths are less than 0.01 cm^{-1} while the spacing between laser lines is ca. 3–4 cm^{-1}. Under these conditions, the point-by-point spectra obtained by using a line tuneable CO laser may not provide an accurate measure of absorption band shapes or the frequency of their maxima. Nevertheless, time-resolved laser absorption allows reaction kinetics to be readily determined. This has been confirmed in several cases by performing kinetic measurements with equivalent results, at two or more points over selected molecular infrared absorption bands. In those cases [e.g., $Cr(CO)_5$ and $Cr(CO)_4$] where a species has more than one accessible infrared transition, identical kinetic results are obtained by monitoring the pressure and temporal dependence of each absorption. The kinetic behavior of a transient absorption feature in conjunction with reported matrix-isolation spectra provides a sound basis for correlating observed transients with particular chemical species.

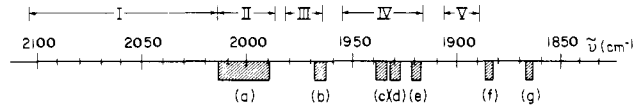

Figure 3. Spectroscopic regions where absorption features are observed following the 249-nm photolysis of $Cr(CO)_6$. Cross-hatched regions have been assigned by Turner and co-workers[5,8] as follows: (a) $Cr(CO)_6$ (t_{1u}); (b) $Cr(CO)_5$ (e); (c) $Cr(CO)_5$ (a_1); (d) $Cr(CO)_4$ (b_1); (e) $Cr(CO)_4$ (a_1); (f) $Cr(CO)_4$ (b_2); (g) $Cr(CO)_3$ (e). Regions labeled with Roman numerals, I–V, denote absorption features observed in the present work (see text).

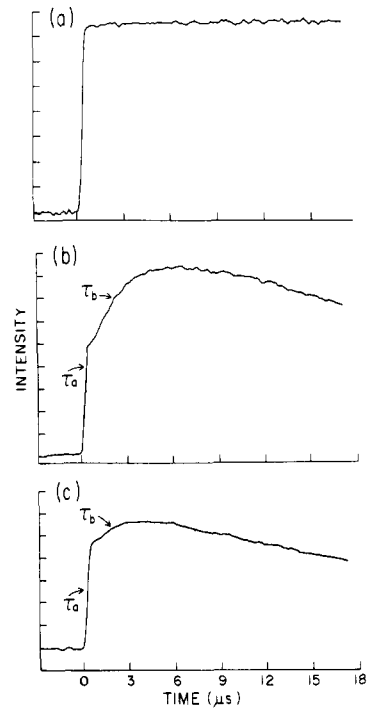

Figure 4. Time-resolved CO (v = 0) absorption following the 249-nm photolysis of $Cr(CO)_6$ for three different sample pressures: (a) 0.050 torr of $Cr(CO)_6$ in 4.0 torr of SF_6; (b) 0.050 torr of $Cr(CO)_6$, neat; (c) 0.010 torr of $Cr(CO)_6$, neat. In parts b and c, τ_a and τ_b are used to label portions of the transient with different rise times (see text).

Carbon Monoxide. Absorptions in region I, 2100–2010 cm^{-1}, are due to CO in vibrational states v = 0–4. If the CO probe laser is tuned to the $P_{v+1,v}(J)$ transition, CO(v,J) will resonantly absorb the incident radiation. The absorption amplitude is determined by the difference in populations for the radiatively coupled states, (v,J) and (v + 1, J − 1). The fact that absorptions in this region are due to CO and not, e.g., $Cr(CO)_6$ or $Cr(CO)_5$ is indicated by the magnitude of the absorption signals ($\alpha_{CO} \sim 1$ cm^{-1} $torr^{-1}$), as well as their pressure and temporal dependences. We conclude that absorptions in region I can be unambiguously assigned to the CO photoproduct.

(21) (a) Lewis, K. E.; Golden, D. M.; Smith, G. P. *J. Am. Chem. Soc.* **1984**, *106*, 3905. (b) Bernstein, M.; Simon, J. D.; Peters, K. S. *Chem. Phys. Lett.* **1983**, *100*, 241.

The temporal evolution of CO following the excitation of $Cr(CO)_6$ at 249 nm has an interesting pressure dependence. Representative examples are shown in Figure 4, where the $P_{1,0}(10)$ CO laser line was used to monitor the temporal evolution of CO. In the presence of ca. 4 torr of a buffer gas, e.g., SF_6, the CO absorption grows in at a detector limited rate following the UV laser pulse (Figure 4a) and decays away only on a 10^{-3} s time scale, as a result of diffusion. Qualitatively different behavior is observed at lower pressure, in the absence of buffer gas. For example, the data in Figure 4b were obtained in neat $Cr(CO)_6$ at a pressure of 0.050 torr. The rising portion of the absorption curve can no longer be fit by a single exponential function. In fact, a nonlinear least-squares analysis[22] indicates that in Figure 4b, CO is formed by (at least) two distinct processes. These processes can be characterized by their rise times, τ_a and τ_b ($\tau_a \leq \tau_b$ under all conditions). If the UV and CO laser beams are rigorously collinear, τ_a is found to correspond to the detection system rise time, independent of sample pressure. On the other hand, τ_b is observed to be pressure dependent (see Figure 4c). With increasing pressure, τ_b decreases until $\tau_b = \tau_a$. Concurrently, the apparent relative yield of CO due to the process characterized by τ_b increases. Comparable behavior is observed both in neat $Cr(CO)_6$ and in dilute mixtures of $Cr(CO)_6$ in two different bath gases (see Figure 5). Apparently, two types of CO, differentiable by their temporal and pressure dependences, are formed upon the 249-nm photolysis of $Cr(CO)_6$. It might be suggested that the CO produced with rise time τ_a is the product of $Cr(CO)_6$ photodissociation while the CO formed with rise time τ_b is the product of a bimolecular reaction, e.g., (1), where $n < 6$.

$$Cr(CO)_n + Cr(CO)_6 \rightarrow Cr_2(CO)_{5+n} + CO \qquad (1)$$

However, τ_b is observed to decrease with increasing pressure for *all* added gases, *not* just $Cr(CO)_6$. We conclude that the CO product formed with rise time τ_b cannot be due to a bimolecular association, such as (1).

The energy supplied by a 249-nm photon is more than sufficient to cleave two Cr–CO bonds in $Cr(CO)_6$. The energy in excess of that necessary to cleave a single $Cr(CO)_5$–CO bond, $h\nu - DH°(Cr–CO)$, is ca. 78 kcal/mol and can be partitioned among the dissociation product's vibrational, relative rotational, and relative translational degrees of freedom. The CO product vibrational energy distribution can be determined by laser absorption methods as previously described.[15,16,23] In the present case, however, the apparent vibrational energy distribution must be interpreted with some care. The reason for this is that CO is formed by at least two distinct processes (τ_a and τ_b) and a characteristic vibrational energy distribution can be anticipated for each. The measured vibrational energy distribution will consist of contributions from each process. In principle, it is possible to deconvolute the measured distribution to obtain distributions corresponding to each of the processes, τ_a and τ_b, but we have not yet attempted this. Nevertheless, by comparing absorption amplitudes measured by using the (1,0) and (2,1) CO laser transitions, we can *qualitatively* conclude that ca. 70% of the total CO product is formed in its ground vibrational state.

Our CO probe laser oscillates on $P_{v+1,v}(J)$ transitions where typically, $J = 8$–13. If the nascent CO product is rotationally excited with $J > 13$, collisional relaxation is required before the CO can be detected by laser absorption. The pressure-dependent rise times τ_b correspond to rate constants $(p\tau_b)^{-1} \sim 8.7 \times 10^6$, 1.9×10^6, and 3.4×10^5 torr^{-1} s^{-1} for $Cr(CO)_6$, SF_6, and argon, respectively, (obtained from the data in Figure 5) which are of the order of magnitude anticipated for CO rotational relaxation. These rate constants do not correspond to any well-defined $J \rightarrow J'$ process but rather to the rate at which the "hot" distribution of CO rotational states is thermalized. We have previously observed pressure-dependent absorption rise times attributable to product rotational excitation in studies of the photodissociation

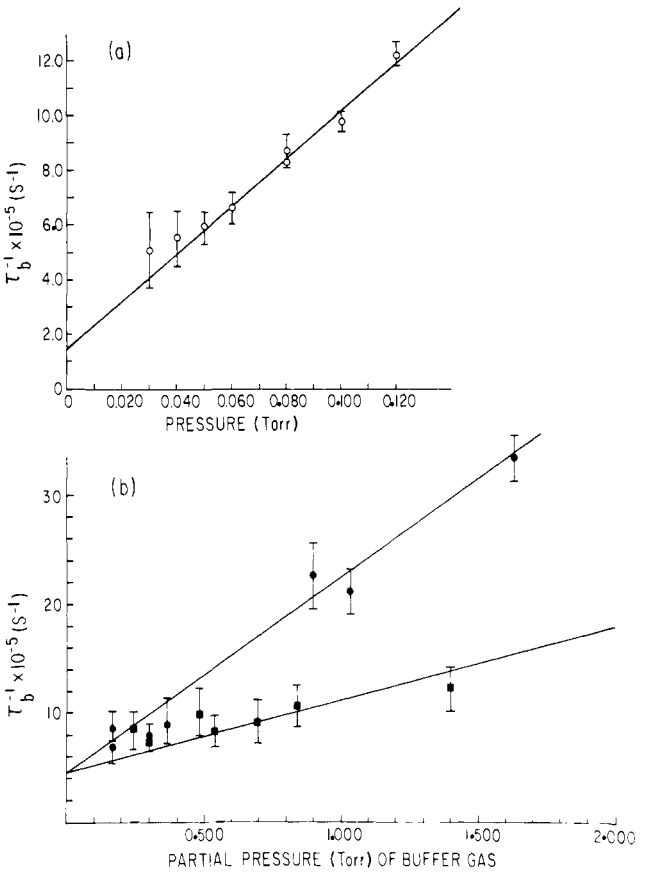

Figure 5. Pressure dependence of τ_b: (a) neat $Cr(CO)_6$; (b) 0.050 torr of $Cr(CO)_6$ in argon (■) and SF_6 (●). Solid lines are least-squares fits to the data.

dynamics of other molecules.[15,16,24] It might be suggested that the yield of CO corresponding to the process with rise time τ_a reflects the *total* yield of nascent CO in the (v,J) state probed by the CO laser.[25] This does not appear to be the case, however. We show below that $Cr(CO)_4$ is produced at a detector limited rate when $Cr(CO)_6$ is photolyzed at 249 nm. Thus, two molecules of CO must be produced at a detector limited rate following the photoactivation of $Cr(CO)_6$. There is no reason to expect the two CO molecules to have similar translational or ro-vibrational energy distributions. The two apparent rates or rise times for CO production shown in parts b and c of Figure 4 correspond to the two sequential decarbonylation reactions which occur as $Cr(CO)_4$ is formed from $Cr(CO)_6$.

Examples of time-dependent CO absorption signals at long times following photoactivation are presented in Figure 6. In the presence of ca. 20 torr of buffer gas, the CO absorption decay can be represented by a single exponential function with a decay time $\tau \sim 10^{-2}$ s (Figure 6a). This is simply the time required for 300 K CO to diffuse out of the volume probed by the CO laser. With decreasing pressure, the CO absorption decay becomes biexponential (Figure 6b) with two decay times, τ_c and τ_d, characterizing the CO loss processes. CO may be removed from the volume probed by the CO laser by chemical reaction, e.g., recombination with a coordinatively unsaturated metal carbonyl, or by a physical process, e.g., diffusion. Both τ_c and τ_d are found to increase with pressure, an observation inconsistent with loss by recombination. With increasing pressure, τ_c increases much faster than τ_d and at sufficiently high pressures (cf. Figure 6a), the two loss precursors are no longer resolvable from one another. Apparently, CO loss is the result of two distinct physical processes. These two loss processes can be related to the two modes of CO

(22) Ruckdeschel, F. R. "BASIC Scientific Subroutines"; BYTE/McGraw-Hill: New York, 1981; Vol. II.
(23) Houston, P. L.; Moore, C. B. *J. Chem. Phys.* **1976**, *65*, 757.
(24) Sonobe, B. I.; Rosenfeld, R. N., unpublished results.
(25) In this case, τ_b^{-1} would correspond to the rate at which this nascent population is (rotationally) relaxed.

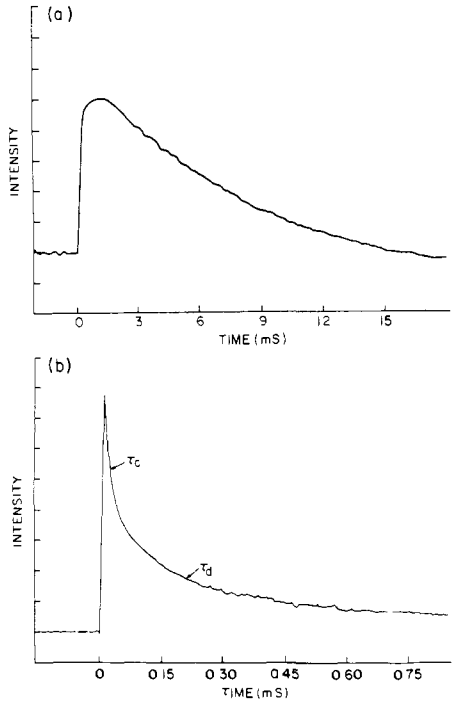

Figure 6. CO (v = 0) absorption at longer times following the 249-nm photolysis of $Cr(CO)_6$: (a) 0.060 torr of $Cr(CO)_6$ in 20 torr of argon; (b) 0.050 torr of $Cr(CO)_6$, neat. τ_c and τ_d are used to label portions of the transient with different decay times (see text).

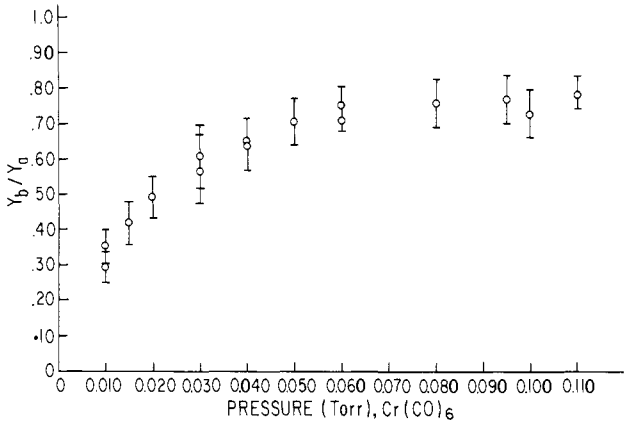

Figure 7. Pressure dependence of the yield of the decarbonylation process characterized by τ_b,Y_b, relative to the yield for that characterized by τ_a,Y_a. These data were obtained by using the $P_{1,0}(10)$ CO laser line. With increasing pressure, the data become approximately constant, $Y_b/Y_a \simeq 0.7$, reflecting the fact that only ca. 70% of the CO product formed following the photolysis of $Cr(CO)_6$ is in v = 0.

formation, characterized by τ_a and τ_b, as follows. The apparent relative yield[26] of CO due to the processes characterized by τ_b is pressure dependent as indicated in parts b and c of Figure 4 and shown explicitly in Figure 7. The CO formed at a detector limited rate ($\tau_a^{-1} \sim 10^7$ s^{-1}) cannot be highly rotationally excited while the CO formed with the slower rise time, τ_b, is rotationally hot prior to any collisional relaxation. Note that (at least partial) collisional relaxation must occur in order for the CO formed with τ_b to be observed by laser absorption. If this CO is ejected from the volume probed by the CO laser prior to collisional relaxation, its *apparent* yield will decrease. This suggests that the rotationally excited CO formed by the photodissociation of $Cr(CO)_6$ at 249 nm is *also* translationally excited, initially. The fast decay, τ_c, thus corresponds to the rate of loss of translationally hot CO from the volume probed by the CO laser. The fact that this fast decay can be observed indicates that the CO is not translationally thermalized even after partial rotational relaxation has occurred. The CO formed with rise time τ_a is rotationally and translationally cold. It diffuses from the volume probed by the CO laser beam in a time τ_d, which corresponds to that expected for the diffusion of CO at 300 K.

The most reasonable explanation for these results is that CO is formed by two processes, (2) and (3): the photodissociation of $Cr(CO)_6$, yielding CO and $Cr(CO)_5$, and the "thermal" dissociation of $Cr(CO)_5$ to yield CO and $Cr(CO)_4$. The photo-

$$Cr(CO)_6 \xrightarrow{249\ nm} CO^{\dagger} + Cr(CO)_5^* \quad (2)$$

$$Cr(CO)_5^* \rightarrow CO + Cr(CO)_4 \quad (3)$$

dissociation, (2), yields ro-vibrationally and translationally excited carbon monoxide, $CO^{\dagger}$, and vibrationally excited chromium pentacarbonyl, $Cr(CO)_5^*$. The extent of vibrational excitation in the $CO^{\dagger}$ product is qualitatively[27] $N_0/\sum_i N_i \simeq 0.4$, where N_i is the relative population in the vibrational state, $v = i$. The $Cr(CO)_5^*$ product is sufficiently excited to undergo further dissociation, yielding products which are relatively cold. Thus, the $CO^{\dagger}$ produced in (2) is observed to grow in with a slow rise time, τ_b, as a result of its rotational excitation and decay away rapidly, in time τ_c, due to its translational excitation. The colder CO produced in (3) grows in rapidly, in time τ_a, indicating it is rotationally relaxed and decays slowly, in time τ_d, since it is translationally thermalized. Although we cannot rigorously rule out the possibility that (3) may be a photoactivated process. rather than the "thermal" fragmentation indicated, the latter case appears more likely. Virtually all of the rotationally cold CO produced following the 249-nm excitation of $Cr(CO)_6$ is in v = 0. The $Cr(CO)_4$ product is stable with respect to unimolecular decay (vide infra). This suggests that relatively little energy (<23 kcal/mol) is available to the products in (3). If this reaction were photoactivated, the large available energy (ca. 68 kcal/mol) would certainly result in the subsequent dissociation of $Cr(CO)_4$, yielding $Cr(CO)_3$. Since no indication of $Cr(CO)_4$ fragmentation is observed, we conclude that (3) is a vibrationally activated process.

Translational excitation in the CO produced via (2) might be further characterized by reducing the CO laser beam diameter until it is smaller than the mean free path in our absorption cell. Under these conditions, the loss rate, τ_c^{-1}, would more nearly reflect the velocity of the nascent CO. However, since the CO is also rotationally excited, collisions are required to observe it with our CO laser. At best we can infer the velocity of CO after it has undergone a few gas kinetic collisions. The result represents only a lower limit to the velocity of the nascent CO. For a sample pressure of 0.050 torr and a CO laser beam diameter of 3 mm, the rapid component of CO loss occurs at a rate $\tau_c^{-1} \sim 1.5 \times 10^6$ s^{-1}. If, on average, a CO molecule must travel a distance on the order of one-half the laser beam diameter to leave the detector zone, its velocity must be ca. 2×10^5 cm/s. The CO will experience at least one gas kinetic collision during the time spent in the detection zone, and this crude velocity estimate does not account for the effect of any elastic or inelastic collisions which might occur. The fractional energy lost by CO per gas kinetic collision with $Cr(CO)_6$ is given by (4), where m_{CO} and m_{MC} are

$$\Delta E/E = 2m_{CO}m_{MC}/(m_{CO} + m_{MC})^2 \quad (4)$$

(26) The relative yields of CO due to τ_a and τ_b at pressure higher than 0.050 torr were obtained by linear least-squares fits to the two linear regions in the semilog plots of time vs. amplitude. Similar results (±10%) were also obtained by measuring the apparent contributions due to τ_a and τ_b suggested by the obvious inflection points present or by use of a nonlinear least-squares curve-fitting routine.[22] At pressures less than 0.050 torr, because CO loss due to translational processes competes with rotational relaxation, semilog plots no longer consist simply of two linear regimes. At these pressures, relative yields were obtained by directly measuring the amplitudes at the inflection points. Similar yields (±15%) are also obtained if the rate constant for rotational relaxation obtained at higher $Cr(CO)_6$ pressures is used (Figure 5a) and then back extrapolated to t = 0 to obtain the relative yields for the processes corresponding to τ_a and τ_b.

(27) This estimate follows from the assumption that essentially all of the CO produced via (3) is in v = 0 and the observation that ca. 70% of the *total* CO produced, i.e., as a result of (2) and (3), is in v = 0.

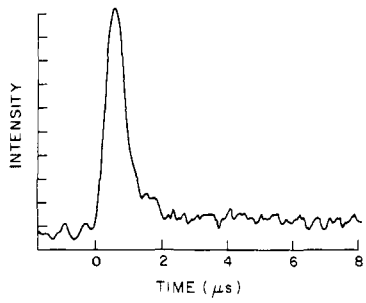

Figure 8. Transient absorption due to $Cr(CO)_4$ at 1900.4 cm^{-1} following the 249-nm photolysis of 0.050 torr of $Cr(CO)_6$ in 0.500 torr of CO and 8.4 torr of He.

the molecular weights of CO and $Cr(CO)_6$, respectively. This suggests that the kinetic energy of the nascent CO produced via (2) must be (at least) ca. 15 kcal/mol. The kinetic energy of the CO produced via (3) is more than an order of magnitude smaller.

Chromium Tetracarbonyl. Absorption due to $Cr(CO)_4$ is anticipated in region V (Figure 3), 1890–1908 cm^{-1}, on the basis of the matrix isolation studies of Turner and co-workers.[8a,b] They observed an absorption at ca. 1896 cm^{-1} in an argon matrix which was assigned as a $\nu_{CO}(b_2)$ vibration of the C_{2v} $Cr(CO)_4$ species. We observe a transient in the range 1895–1910 cm^{-1} (Figure 8) that has detector limited rise time. Its decay can be fit with a single exponential function. Since the CO absorption bands of metal carbonyls are typically red shifted in an argon matrix relative to the gas phase, our assignment of the transient to $Cr(CO)_4$ is consistent with the assignment made by Turner and co-workers.[8a,b] If the photolysis of $Cr(CO)_6$ is carried out in the presence of added CO, the $Cr(CO)_4$ absorption is found to decay at a rate proportional to the pressure of added CO (vide infra). This indicates that the transient observed here is an unsaturated metal carbonyl. Absorption features which have temporal and pressure dependences identical with the feature observed in region V are also observed in region IV. Because the former overlap to some extent with $Cr(CO)_5$ absorption bands, quantitative kinetic studies were carried out by using the region V transient. However, the fact that the transients observed are all nearly coincident with the $Cr(CO)_4$ bands reported by Turner and co-workers[8] provides good evidence that our assignment of these features to $Cr(CO)_4$ is correct.

Yardley and co-workers[4] have reported that when a mixture of $Cr(CO)_6$ and PF_3 is photolyzed at 249 nm, one of the products isolated is $Cr(CO)_3(PF_3)_3$. They thus infer that $Cr(CO)_3$ is produced by the photolysis and subsequently undergoes three sequential association reactions with PF_3. An absorption band for $Cr(CO)_3$ is anticipated near 1867 cm^{-1}, based on the matrix isolation studies of Turner and co-workers[8a] (Figure 3). We have conducted a systematic search for transients in the region 1890–1830 cm^{-1}. No absorption could be detected in this range. This indicates that the $Cr(CO)_4$ formed following the 249-nm photolysis of $Cr(CO)_6$ is stable with respect to unimolecular decay. Moreover, if $Cr(CO)_4$ was formed by the association reaction, (5), the rise time of the $Cr(CO)_4$ absorption would depend on CO pressure.

$$Cr(CO)_3 + CO \rightarrow Cr(CO)_4 \qquad (5)$$

We find that the rise time of the $Cr(CO)_4$ signal is detector limited, independent of the pressure of CO [for $p(CO) = 0$–5 torr] or any other reagent. Even if reaction 5 has no activation barrier, the 100-ns response time of our detection system would be more than sufficient to resolve the rate of $Cr(CO)_4$ formation due to (5) under low-pressure conditions (e.g., $p[Cr(CO)_6] \simeq 0.05$ torr, $p(CO) \simeq 0.2$ torr). We conclude that $Cr(CO)_4$ is the major fragment produced upon the 249-nm photolysis of $Cr(CO)_6$ and that it is produced via the sequential unimolecular reactions 2 and 3. If any $Cr(CO)_3$ is formed, its yield is less than 10% of the yield of $Cr(CO)_4$ based on our detection sensitivity. This conclusion has some interesting thermochemical implications. The 249-nm photons have an energy of 115 kcal/mol. $DH°[(CO)_5Cr\text{-}CO]$ is ca. 37 kcal/mol[21] while $DH°[(CO)_4Cr\text{-}CO]$ has been estimated to be ca. 40 kcal/mol.[21] Thus, the maximum internal energy remaining in the $Cr(CO)_4$ fragment is 38 kcal/mol. Since >15 kcal/mol of energy is partitioned to CO translational and rovibrational degrees of freedom in (2), the energy of the $Cr(CO)_4$ fragment formed via (3) must be <23 kcal/mol. Reaction 6 is endothermic[28] by 156 kcal/mol, so ca. 79 kcal/mol are required to remove the four ligands from $Cr(CO)_4$. The average Cr–CO bond energy in $Cr(CO)_4$ is ca. 20 kcal/mol. Thus, the internal energy of the $Cr(CO)_4$ fragment is, on average, likely to be insufficient for dissociation to $Cr(CO)_3$. If reaction 7 was the primary mode of decay for $Cr(CO)_4$, the $Cr(CO)_4$ loss rate would decrease with increasing pressure. In fact, precisely the opposite

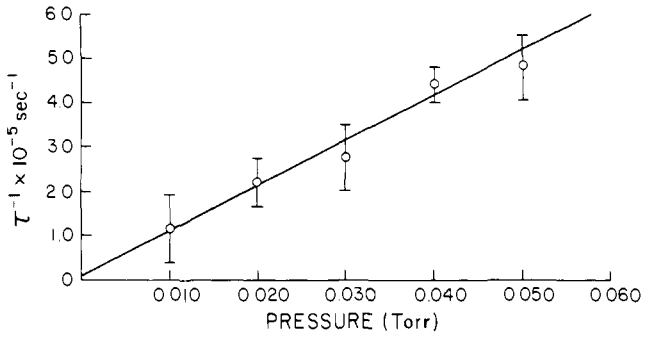

Figure 9. Dependence of the $Cr(CO)_4$ decay rate on the pressure of $Cr(CO)_6$. The solid line is a least-squares fit to the data.

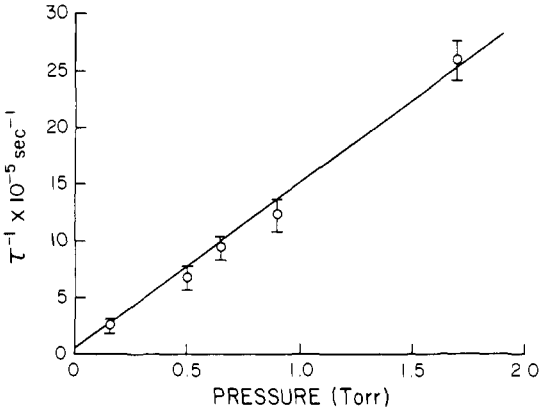

Figure 10. Dependence of the $Cr(CO)_4$ decay rate on the pressure of CO. The solid line is a least-squares fit to the data.

$$Cr(CO)_6 \rightarrow Cr + 6CO \qquad (6)$$

$$Cr(CO)_4^* \xrightarrow{k_7} Cr(CO)_3 + CO \qquad (7)$$

is observed. As the pressure of an added gas, L, is increased, the rate of $Cr(CO)_4$ loss is found to increase. This indicates that the primary mode of decay for $Cr(CO)_4$ is via association, (8), where L = CO or SF_6. In the absence of any added gas, $Cr(CO)_4$ decays

$$Cr(CO)_4 + L \rightarrow Cr(CO)_4L \qquad (8)$$

by association with $Cr(CO)_6$, eq 9. The pressure dependence of

$$Cr(CO)_4 + Cr(CO)_6 \xrightarrow{k_9} Cr_2(CO)_{10} \qquad (9)$$

the rate of $Cr(CO)_4$ decay in neat $Cr(CO)_6$ is shown in Figure 9. These data were obtained by monitoring the $Cr(CO)_4$ absorption at 1900.4 cm^{-1}, but identical results, within our experimental error, are obtained by monitoring the $Cr(CO)_6$ absorption at 1995.1 cm^{-1} (vide infra). $Cr(CO)_4$ undergoes association with $Cr(CO)_6$ with a rate constant $k_9 = 1.8 (\pm 0.3) \times 10^7$ $torr^{-1}$ s^{-1}.

(28) (a) Connor, J. A. *Top. Curr. Chem.* **1977**, *71*, 71. (b) Cotton, F. A.; Fischer, A. K.; Wilkinson, G. J. *J. Am. Chem. Soc.* **1956**, *78*, 5168.

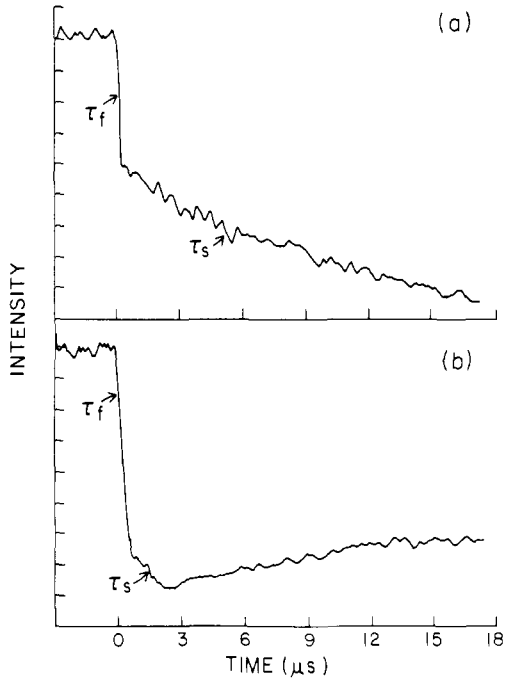

Figure 11. Transient absorption due to $Cr(CO)_6$ at 1995.1 cm^{-1} following photolysis at 249 nm: (a) 0.005 torr of $Cr(CO)_6$, neat; (b) 0.050 torr of $Cr(CO_6)$, neat. τ_f and τ_s are used to label portions of the transients with different decay times.

$Cr(CO)_4$ undergoes gas kinetic collisions with $Cr(CO)_6$ at a rate of ca. $1-2 \times 10^7$ $torr^{-1}$ s^{-1}. Therefore, reaction 9 occurs on virtually every collision and has a negligible activation barrier. We find that $Cr(CO)_4$ recombines with CO, eq 10, at an apparently slower rate. By measuring the rate of $Cr(CO)_4$ decay as a function of

$$Cr(CO)_4 + CO \xrightarrow{k_{10}} Cr(CO)_5 \qquad (10)$$

CO pressure, Figure 10, we find $k_{10} \simeq 1.4\ (\pm 0.2) \times 10^6$ $torr^{-1}$ s^{-1}. Thus, reaction 10 occurs on only one in ten gas kinetic collisions, indicating the reaction rate may not be in the high-pressure limit. (**Note Added in Proof**: This has been confirmed by recent experiments in our laboratory.)

Chromium Hexacarbonyl. The $\nu_{CO}(t_{1u})$ vibration of $Cr(CO)_6$ occurs near 2000 cm^{-1}, region II. The CO laser absorption amplitude in this region is proportional to the concentration of $Cr(CO)_6$. Depletion of $Cr(CO)_6$ as a result of photodissociation results in a transient increase in the CO laser intensity reaching the infrared detector. Typical data are shown in Figure 11. At $t < 18$ μs, it is apparent that the concentration of $CrCO)_6$ is depleted by two processes. The first of these is characterized by a detector limited decay time, τ_f, independent of sample pressure and is due to the photodissociation of $Cr(CO)_6$. The second process which consumes $Cr(CO)_6$ has a slower decay time, τ_s, which is dependent on the pressure of $Cr(CO)_6$. The pressure dependence of τ_s is illustrated in Figure 12. This slower loss process has a rate constant of 2.2 $(\pm 0.4) \times 10^7$ $torr^{-1}$ s^{-1}. This rate constant is the same, within our experimental error, as the rate constant, k_9, for $Cr(CO)_4$ consumption in neat $Cr(CO)_6$ [see eq 9]. Therefore, we make the assignment $(p\tau_s)^{-1} \equiv k_9$, i.e., the slower loss process, τ_s, results from $Cr(CO)_4$–$Cr(CO)_6$ clustering. This clustering reaction can be almost completely suppressed in the presence of added CO. This is demonstrated in Figure 13. The dependence of the rate of recovery of the $Cr(CO)_6$ absorption on CO pressure is shown explicitly in Figure 14, which yields a rate constant $k_{13} = 1.2\ (\pm 0.2) \times 10^6$ $torr^{-1}$ s^{-1}. Within our experimental uncertainty, this is the same as the rate constant for $Cr(CO)_5$ decay in the presence of added CO (vide infra). On this basis, we conclude that in the presence of added CO, $Cr(CO)_6$ is regenerated via 11. In the absence of added CO, little re-

$$Cr(CO)_5 + CO \xrightarrow{k_{11}} Cr(CO)_6 \qquad (11)$$

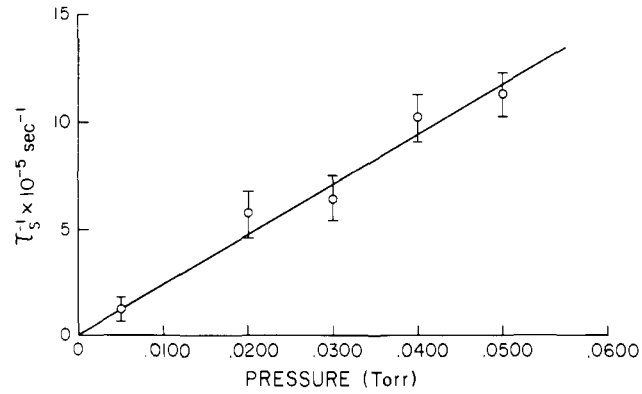

Figure 12. Dependence of τ_s^{-1} on the pressure of $Cr(CO)_6$. The solid line is a least-squares fit to the data.

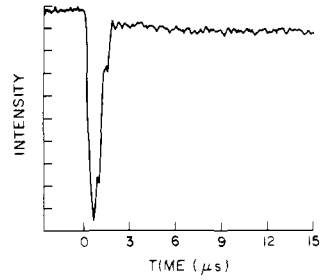

Figure 13. Transient absorption due to $Cr(CO)_6$ at 1995.1 cm^{-1} following photolysis at 249 nm: $p[Cr(CO)_6] = 0.010$ torr, $p(CO) = 1.8$ torr, and $p(He) = 7.2$ torr. Complete recovery of the absorption to base line is not observed because of the competing clustering reaction.

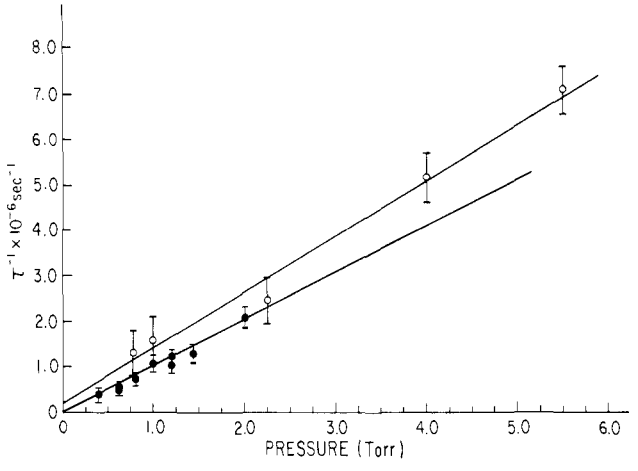

Figure 14. Dependence of the rate at which the $Cr(CO)_6$ absorption recovers on the pressure of added CO. The solid lines are least-squares fits to the data. Data represented by an open circle were obtained by monitoring the $Cr(CO)_6$ absorption at 1995.1 cm^{-1} while data represented by a solid circle were obtained by monitoring the $Cr(CO)_5$ absorption at 1977.4 cm^{-1}. The respective rate constants are 1.2×10^6 and 9.6×10^5 $torr^{-1}$ s^{-1}.

generation of $Cr(CO)_6$ is observed since $k_9 \gg k_{10}$, k_{11}, but with sufficient CO pressure, e.g., Figure 13, virtually complete regeneration of $Cr(CO)_6$ occurs.

Chromium Pentacarbonyl. An absorption band due to $Cr(CO)_5$ is anticipated near 1980 cm^{-1} (region III, Figure 3). This corresponds to a $\nu_{CO}(e)$ vibration of the ground state[8c,d] C_{4v} $Cr(CO)_5$. Upon the photolysis of $Cr(CO)_6$ at 249 nm two transient absorption features are observed near 1980 cm^{-1}. These features can be resolved from one another as a result of their qualitatively different pressure dependences (Figure 15). In the absence of added CO, a single feature is observed whose rise time depends on $[Cr(CO)_6]$ and which decays on a 10^{-3} s time scale (Figure 15a). This feature cannot be due to $Cr(CO)_5$ because both its rise and decay times are independent of CO pressure. It can be

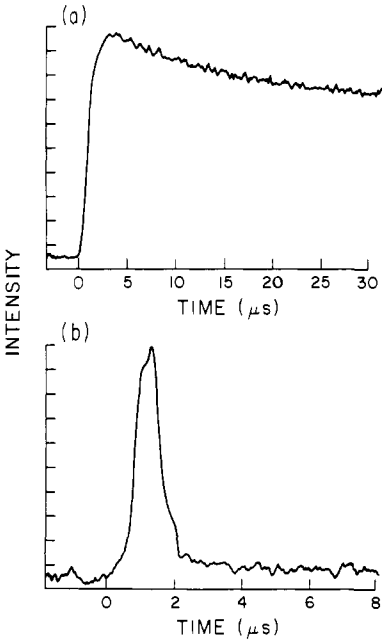

Figure 15. Time-resolved absorption at 1977.4 cm^{-1} following the 249-nm photolysis of $Cr(CO)_6$: (a) $p[Cr(CO_6)]$ = 0.060 torr and p(He) = 9 torr; (b) $p[Cr(CO)_6]$ = 0.015 torr, p(CO) = 1.0 torr, and p(He) = 8 torr.

assigned to the binuclear species $Cr_2(CO)_{10}$ as described below. In the presence of added CO (Figure 15b), an additional feature is observed whose rise and decay times depend on CO pressure and whose relative amplitude increases with increasing CO pressure. The decay time for this feature can be characterized by a rate constant, $(p\tau)^{-1} = 9.6 \times 10^5$ $torr^{-1}$ s^{-1}, which is identical, within experimental error, with k_{11}, the rate constant for $Cr(CO)_6$ regeneration (see Figure 14). Signals with comparable kinetic behavior are also observed in region IV (Figure 3) but overlap $Cr(CO)_4$ signals in this region, to some extent. Thus, kinetic measurements were performed by using the region III transient. The near coincidence of the transients observed in these two regions with reported $Cr(CO)_5$ absorption bands[8] and their pressure-dependent kinetic behavior supports the assignment of these transients to $Cr(CO)_5$. It might be anticipated that the $Cr(CO)_5$ transient should grow in with a rate constant equivalent to k_{10}, the rate constant for $Cr(CO)_4$ decay in the presence of CO. This is not the case when the total pressure is $\lesssim$10 torr. The growth of the $Cr(CO)_5$ transient, while qualitatively dependent on CO pressure, cannot be fit by a simple exponential function or by a sum of two exponentials. Thus a kinetic scheme for the $Cr(CO)_n$ system which includes *only* reactions 10 and 11 cannot account for the appearance rate of $Cr(CO)_5$. A more complex scheme, perhaps involving metastable intermediates [e.g., C_{2v} or high-spin D_{3h} isomers of $Cr(CO)_5$], may be operative, but available data do not presently permit the hypothesis to be evaluated further.

It should be noted that *no* $Cr(CO)_5$ is observed immediately following the photolysis of $Cr(CO)_6$ at 249 nm. $Cr(CO)_5$ can be observed only in the presence of added CO, as a result of reaction 10. This is because the nascent $Cr(CO)_5$ product of (2) contains sufficient internal energy to dissociate, reaction 3, prior to collisional stabilization. The lifetime of the nascent $Cr(CO)_5$ product is ca. 10^{-9} s, as estimated by quantum-RRK theory.[29] Thus, pressures $\gtrsim 10^3$ torr are required for its collisional stabilization. This result indicates that, while $Cr(CO)_5$ might be observed as a primary product of the *solution phase* photolysis of $Cr(CO)_6$ at 249 nm, it will not be detected as a primary product in gas-phase experiments (at sub-atmospheric pressures) with nanosecond temporal resolution. A possible approach for directly generating $Cr(CO)_5$ in the gas phase would be via the photolysis of $Cr(CO)_6$ at a wavelength of ca. 350 nm. In this case, the internal energy of the nascent $Cr(CO)_5$ should be insufficient for further fragmentation to occur. Investigations along these lines are currently underway.

Binuclear Complexes. The kinetic data detailed above provide strong evidence that binuclear chromium complexes can be formed following the 249-nm photolysis of $Cr(CO)_6$ in the gas phase. In particular, this is confined by (i) the $[Cr(CO)_6]$ dependence of the $Cr(CO)_4$ decay rate (Figure 9) and (ii) the $[Cr(CO)_6]$ dependence of the secondary, i.e., following photodissociation, $Cr(CO)_6$ decay rate (Figure 12). Since no CO formation is observed on the time scale of binuclear complex formation, we conclude the complex formed must be $Cr_2(CO)_{10}$. A transient absorption is observed near 1980 cm^{-1} (Figure 15a) whose rise time, τ_i, is dependent on $[Cr(CO)_6]$. The corresponding rate constant is $(p\tau_i)^{-1} = 1.14 \times 10^7$ $torr^{-1}$ s^{-1}. Within our experimental error, $(p\tau_i)^{-1} = (p\tau_s)^{-1} = k_9$, i.e., identical rate constants for $Cr_2(CO)_{10}$ formation are obtained by monitoring the absorption lines of $Cr(CO)_4$, $Cr(CO)_6$, and $Cr_2(CO)_{10}$. This suggests that the absorption feature observed near 1980 cm^{-1}, in the absence of CO, corresponds to $Cr_2(CO)_{10}$. The conclusion that $Cr_2(CO)_{10}$ is formed by the reaction of $Cr(CO)_4$ with $Cr(CO)_6$, (9), is significant in part because there are very few reported cases of neutral binuclear chromium complexes in the literature. Our data indicate that $Cr_2(CO)_{10}$ can be generated in the gas phase under conditions where it is stable for times on the order of at least 10^{-3} s. A broad infrared absorption feature for this complex is observed near 1980 cm^{-1}. The occurrence of an infrared transition for $Cr_2(CO)_{10}$ near 1980 cm^{-1}, i.e., in the vicinity of the $Cr(CO)_5$ ν_{CO}(e) vibration, suggests, but does not require, that the structure of the binuclear complex may resemble to some extent a pair of interacting $Cr(CO)_5$ moieties.

It is perhaps somewhat surprising that $Cr_2(CO)_{10}$ is formed on every collision of $Cr(CO)_4$ with $Cr(CO)_6$, i.e., there is no barrier to its formation. Direct formation of a Cr–Cr bond in this reaction seems unlikely since a relatively unprecedented seven-coordinate chromium species, $(CO)_6Cr–Cr(CO)_4$, would necessarily be generated. An alternative possibility involves the initial formation of an oxygen-bonded complex, I, or a doubly bridged species, II, either of which may undergo rapid isomerization to a Cr–Cr bonded cluster, (12). The data presently available do not provide

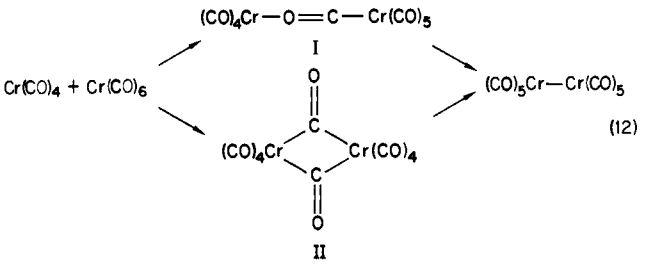

(12)

a basis for any firm conclusions to be drawn, however, either on the structure of the species, $Cr_2(CO)_{10}$, or its mechanism of formation.

Overview. The results reported here allow a relatively simple model to be constructed for the photochemistry of $Cr(CO)_6$ following 249-nm excitation. This model is summarized in Scheme I, where the asterisk denotes vibrational excitation. Both dis-

Scheme I

$$Cr(CO)_6 \xrightarrow{249\ nm} [Cr(CO)_5]^* + CO \quad (2)$$

$$[Cr(CO)_5]^* \rightarrow Cr(CO)_4 + CO \quad (3)$$

$$Cr(CO)_4 + Cr(CO)_6 \xrightarrow{k_9} Cr_2(CO)_{10} \quad (9)$$

$$Cr(CO)_4 + CO \xrightarrow{k_{10}} Cr(CO)_5 \quad (10)$$

$$Cr(CO)_5 + CO \xrightarrow{k_{11}} Cr(CO)_6 \quad (11)$$

(29) Robinson, P. J.; Holbrook, K. A. "Unimolecular Reactions"; Wiley-Interscience: New York, 1972.

sociative steps, (2) and (3), occur at a detector limited rate, i.e., $\geq 10^7$ s^{-1}. This model differs from that which we have previously proposed[6] where a long-lived excited state of $Cr(CO)_6$ was suggested as a precursor to $Cr(CO)_5$ on the basis of an apparently slow CO production rate. In our preliminary studies, mechanistic conclusions were drawn solely on the basis of time-resolved studies of CO: unsaturated metal carbonyls were not directly observed. Subsequent work has shown that some of the "structure" initially found in the [CO] temporal dependence was due to misalignment of the photolysis and probe laser beams. Careful attention to laser alignment yields data, e.g., Figure 1, which show no evidence for slow production of CO. Direct observation of $Cr(CO)_4$ and $Cr(CO)_5$ also demonstrates that all dissociative processes occur within 10^{-7} s following excitation of $Cr(CO)_6$ at 249 nm. We conclude that Scheme I is the simplest kinetic model consistent with all our time-resolved absorption data.

Studies of the photochemistry of $Cr(CO)_6$ in condensed phases have generally led to the conclusion that single ligand cleavage, (13), is the dominant dissociative event.[1] Similar conclusions

$$Cr(CO)_6 \xrightarrow{h\nu} Cr(CO)_5 + CO \qquad (13)$$

were reached by Breckenridge and Sinai,[9] who examined the 355-nm photochemistry of $Cr(CO)_6$ in the gas phase. At this excitation wavelength, cleavage of more than one metal–CO bond is unlikely due to the available energy. In several cases,[3,11,14] it was noted that $Cr(CO)_5$ is highly reactive, undergoing rapid association with nominally inert solvents or added gases. Studies by Yardley and co-workers,[4] as well as Grant and co-workers,[2] have suggested that polyunsaturated species, e.g., $Fe(CO)_3$, can be formed following single photon absorption by $Fe(CO)_5$ near 300 nm. Weitz and co-workers[12] have confirmed this suggestion, using time-resolved infrared absorption spectroscopy to directly observe photofragments. Yardley and co-workers[4] have reported that a distribution of unsaturated species, $Cr(CO)_n$ (n = 2–5), is produced when $Cr(CO)_6$ is irradiated at 249 nm in the gas phase. They reached this conclusion on the basis of studies where PF_3 was used to (presumably) quantitatively trap unsaturated metal carbonyls, i.e., the extent of PF_3 incorporation was taken as an indication of the extent of unsaturation of the photoproducts. The preponderance of evidence thus clearly indicates that highly unsaturated species can be prepared by the photoactivation of metal carbonyls, e.g., $Cr(CO)_6$, in the gas phase, while in condensed phases, only the mono-unsaturated species, $Cr(CO)_5$, is formed, even when the available energy is sufficient to cleave two Cr–CO bonds. One possible solution for this apparent dichotomy of behavior is that, in solution, internal energy in the nascent $Cr(CO)_5$* photoproduct is removed via collisions with solvent faster than decomposition to $Cr(CO)_4$ + CO occurs. Alternatively, cage effects may enhance CO + $Cr(CO)_4$ recombination in solution. Such cage effect might be relatively ineffective in promoting CO + $Cr(CO)_5$ recombination if the CO product of the photodissociation of $Cr(CO)_6$ is translationally hot. However, the observation of quantum yields for dissociation (or photosubstitution) less than unity in solution[30] may indicate the role of cage effects in this case, as well, to some extent. Turner and co-workers[8a] have shown that the production of $Cr(CO)_4$ from $Cr(CO)_6$ requires prolonged photolysis in cryogenic matrices, and it appears that gas-phase photochemical methods offer a more advantageous approach for the generation of highly unsaturated metal centers and the study of their chemistry.

Yardley and co-workers[4] report that the irradiation of $Cr(CO)_6$ at 249 nm in the gas phase yields $Cr(CO)_5$:$Cr(CO)_4$:$Cr(CO)_3$:$Cr(CO)_2$ = 0.03:0.73:0.14:0.10. The present studies demonstrate that the $Cr(CO)_5$ formed via photodissociation, (16), is metastable with a lifetime less than 10^{-7} s. Thermal $Cr(CO)_5$ is formed only via the recombination of $Cr(CO)_4$ with CO, a relatively slow process in the absence of added CO. We find no evidence that species more highly unsaturated than $Cr(CO)_4$ are produced upon the 249-nm photolysis of $Cr(CO)_6$. PF_3 trapping experiments[4] appear to indicate that $Cr(CO)_4$:$Cr(CO)_3$:$Cr(CO)_2$ = 1:0.19:0.14. This suggests the possibility that an association–dissociation mechanism, (19) may be operative in these studies.

$$Cr(CO)_4 + PF_3 \rightleftarrows [Cr(CO)_4PF_3]^* \rightarrow Cr(CO)_3PF_3 + CO \qquad (14)$$

Useful comparisons may be drawn between the kinetic data determined here, for the reactions of $Cr(CO)_4$ and $Cr(CO)_5$, and similar data obtained for other transition-metal carbonyls. Relevant data are summarized in Table I. Unsaturated chromium carbonyls recombine with CO with rate constants comparable to those for unsaturated iron carbonyl/CO recombination. A notable exception to this observation is the reaction $Fe(CO)_4$ + CO → $Fe(CO)_5$, which occurs almost three orders of magnitude more slowly than the other metal carbonyl/CO recombinations. This qualitative difference in reactivity may be due to the nature of the spin multiplicity changes associated with the various recombination reactions. The ground-state spin multiplicities of some transition-metal carbonyls are listed in Table II. The recombination of $Cr(CO)_4$ and $Cr(CO)_5$ with CO can occur with conservation of spin angular momentum. The same is true for the recombination of $Fe(CO)_3$ with CO. These reactions occur at comparable rates. The recombination of $Fe(CO)_4$ with CO to yield ground electronic state $Fe(CO)_5$ is formally a spin-forbidden process. This is reflected in the relatively small rate constant for the reaction.[35] The observation that $Fe(CO)_2$ recombines with CO at a rate comparable to that for $Fe(CO)_3$ and the unsaturated chromium carbonyls suggests that the reaction $Fe(CO)_2$ + CO → $Fe(CO)_3$ occurs with spin conservation. In this case, $Fe(CO)_2$ should be a ground-state triplet. $Cr(CO)_4$ reacts with $Cr(CO)_6$ ca. ten times faster than it reacts with CO. The facility of the $Cr(CO)_4$ + $Cr(CO)_6$ reaction may reflect an increased electron density at the carbonyl oxygens in $Cr(CO)_6$ relative to the electron density at carbon or oxygen in CO, but

Table I. Rate Constants for the Reactions of Coordinatively Unsaturated Metal Carbonyls

reaction	rate constant, $torr^{-1}$ s^{-1}	ref
$Cr(CO)_5$ + CO → $Cr(CO)_6$	1.2 (±0.2) × 10^6	*a*
$Cr(CO)_4$ + CO → $Cr(CO)_5$	1.4 (±0.2) × 10^6	*a*
$Cr(CO)_4$ + $Cr(CO)_6$ → $Cr_2(CO)_{10}$	1.8 (±0.3) × 10^7	*a*
$Fe(CO)_4$ + CO → $Fe(CO)_5$	1.9 × 10^3	12
$Fe(CO)_3$ + CO → $Fe(CO)_4$	6 (±3) × 10^5	31
$Fe(CO)_2$ + CO → $Fe(CO)_3$	8 (±4) × 10^5	31

[a] This work.

Table II. Electronic Structural Data on Transition-Metal Carbonyls

	ground-state geometry	ground-state spin multiplicity[e]
$Cr(CO)_6$	O_h	singlet
$Cr(CO)_5$	C_{4v}[a]	singlet
$Cr(CO)_4$	C_{2v}	singlet
$Fe(CO)_5$	D_{3h}	singlet
$Fe(CO)_4$	C_{2v}[b]	triplet
$Fe(CO)_3$	C_{3v}[c]	triplet
$Fe(CO)_2$	*d*	*d*

[a] Reference 8. [b] Reference 32. [c] Reference 33. [d] No data available. [e] Reference 34.

(30) Nasielski, J.; Colas, A. *Inorg. Chem.* **1978**, *17*, 237.

(31) Ouderkirk, A. J.; Ph.D. Thesis, University Microfilms International, Ann Arbor, MI, 1983.

(32) Poliakoff, M.; Turner, J. J. *J. Chem. Soc., Dalton Trans.* **1974**, 2276.

(33) Poliakoff, M. *J. Chem. Soc., Dalton Trans.* **1974**, 210.

(34) Burdett, J. K. "Molecular Shapes"; Wiley-Interscience, New York, 1980.

(35) Grant and co-workers have recently reported that $Fe(C_2H_4)(CO)_3$ recombines with CO ca. two orders of magnitude more slowly than the corresponding reaction of $Fe(CO)_4$. See: Miller, M. E.; Grant, E. R. *J. Am. Chem. Soc.* **1984**, *106*, 4635.

additional data are required to evaluate this hypothesis.

Conclusions. The time-resolved laser absorption spectroscopic method described here offers a general approach for studying the photodissociation dynamics of transition-metal carbonyls and the spectroscopy and chemical kinetics of the coordinatively unsaturated species formed as a result of photodissociation. In the present article, we have applied this method in characterizing the primary and secondary processes which occur following the photoactivation of $Cr(CO)_6$ at 249 nm.

Our results demonstrate that photoactivated $Cr(CO)_6$ rapidly decays to $Cr(CO)_5$ and CO. The nascent CO product is translationally, as well as rovibrationally, excited, and the $Cr(CO)_5$ product is formed with sufficient internal energy to decay to $Cr(CO)_4$ and CO. Both dissociation reactions occur within 10^{-7} s after the photoactivation step. The $Cr(CO)_4$ and CO formed via the unimolecular dissociation of $Cr(CO)_5$ are both relatively cold, and the $Cr(CO)_4$ product is stable with respect to further unimolecular decay. $Cr(CO)_4$ is observed to undergo association with $Cr(CO)_6$ on every gas kinetic collision, forming the binuclear complex $Cr_2(CO)_{10}$. This species is stable to times on the order of at least 10^{-3} s. Both $Cr(CO)_4$ and $Cr(CO)_5$ are found to recombine with CO at a rate corresponding to one in ten gas kinetic collisions, forming $Cr(CO)_5$ and $Cr(CO)_6$, respectively. Our results demonstrate that under appropriate conditions, reactive species such as $Cr(CO)_4$, $Cr(CO)_5$, and $Cr_2(CO)_{10}$ can be generated in the gas phase in yields sufficient for the study of their spectroscopy and kinetics.

Acknowledgment is made to the donors of the Petroleum Research Fund, administered by the American Chemical Society, for partial support of this work. Additional support has been provided by the National Science Foundation through Grant NSF CHE82-06897.

Registry No. $Cr(CO)_6$, 13007-92-6; $Cr(CO)_5$, 26319-33-5; $Cr(CO)_4$, 56110-59-9; $Cr_2(CO)_{10}$, 95387-63-6; CO, 630-08-0.

Molecular Mechanical Studies of Inclusion of Alkali Cations into Anisole Spherands

Peter A. Kollman,* Georges Wipff,† and U. Chandra Singh

Contribution from the Department of Pharmaceutical Chemistry, University of California, San Francisco, San Francisco, California 94143. *Received December 22, 1983*

Abstract: We present molecular mechanical studies of host spherands **1**, **2**, and **3** and their complexes with Li^+, Na^+, and K^+ guests. Even though such an approach is quite simple, we show that it is capable of giving interesting insight into host/guest complexation. Specifically, we calculate a high selectivity of **1** for Li^+ and Na^+ complexation compared to that of K^+, in agreement with experiment. The difference between $-\Delta E$ for complexation of Na^+ compared to K^+ is much larger with **1** (41 kcal/mol) than with 18-crown-6 (**4**) (8 kcal/mol). This dramatic difference clearly shows why **1** has no thermodynamic tendency to bind K^+. Decomplexation of the unsolvated cations from the cavity of **1** has been simulated by moving Li^+, Na^+, and K^+ along the threefold axis out of the molecule; this lead to ~25 kcal/mol higher energies for Li^+ and Na^+ but ~55 kcal/mol higher energy for K^+. Moving the cations further along the axis of **1** and energy refining causes Li^+ and Na^+ to return to the center of the cavity; K^+, on the other hand, remains on the outside of the cavity with an energy 18 kcal/mol lower than that found at the model "transition state". The calculated free energy differences in complexation of Li^+ and Na^+ with **1** and **2** are 13.6 and 15.6 kcal/mol, respectively, qualitatively consistent with the observed free energy differences of >12.6 and 12.6 kcal/mol, respectively. We present normal mode analyses and entropy calculations on **1** and **2** and their complexes, which help to further elucidate the nature of these complexes. Calculations on spherand **3a** lead to a relative free energy of Li^+ complexation which is qualitatively consistent with the experimental observation that the complexation free energy of **3a** is between that of **1** and **2**. Another conformation of this molecule, **3b**, is calculated to have a higher Li^+ affinity even than **1**, which has the highest experimentally observed Li^+ affinity. This conformation is calculated to be much more stable than **3a**, and reaction pathway calculations suggest that **3a** is a kinetically trapped conformation. These predictions have been borne out by experiments (see Note Added in Proof).

Spherands are very interesting ionophores, which differ from crowns, cryptands, and natural ionophores in that they are "fully organized" for cation complexation during synthesis rather than undergoing conformational changes in the presence of cation. Cram et al.,[1,2] Lein and Cram,[3] and Trueblood et al.[4] have presented the synthesis, thermodynamics, and kinetics of binding and X-ray crystal structures of a number of spherands and have demonstrated that spherand **1** has the highest binding affinity for Li^+ and Na^+ of this class of structures, larger than the affinity of the best simple cryptand binders for Li^+ and Na^+ (by $\sim 10^4$ and 10^2, respectively[2]). The rather dramatic difference in affinity of Li^+ and Na^+ for **1** compared to **2** is also interesting; replacement of a single OCH_3 by H reduces the association constant for binding of cation by $\sim 10^9$ for both cations. Another very interesting result is the complete lack of (measurable) affinity of **1** for K^+, in that **1** will extract trace amounts of Na^+ and Li^+ from reagent grade KOH when mixed with that base.[1]

We have been interested in modeling cation–ionophore interactions for some time and have recently presented the first extensive molecular mechanics study[5] of an ionophore *and* its cation complexes. The results of that study were encouraging, in that a rather simple simple model was able to account for the relative stabilities of 18-crown-6 conformations in the absence of cation

† Institut de Chimie, BP 296/R8, 67008 Strasbourg, France.

(1) Cram, D. J.; Kaneda, T.; Helgeson, R. C.; Lein, G. M. *J. Am. Chem. Soc.* **1979**, *101*, 6752.
(2) Cram, D. J.; Lein, G. M.; Kaneda, T.; Helgeson, R. C.; Knobler, C. B.; Maverik, E.; Trueblood, K. N. *J. Am. Chem. Soc.* **1981**, *103*, 6228.
(3) Lein, G. M.; Cram, D. J. *J. Chem. Soc., Chem. Commun.* **1982**, 301.
(4) Trueblood, K. N.; Knobler, C. B.; Maverick, E.; Helgeson, R. C.; Brown, S. B.; Cram, D. J. *J. Am. Chem. Soc.* **1981**, *103*, 5594.
(5) Wipff, G.; Weiner, P.; Kollman, P. *J. Am. Chem. Soc.* **1982**, *104*, 3249.

0002-7863/85/1507-2212$01.50/0 © 1985 American Chemical Society